Mechanics & Industry **21**, 208 (2020)
© AFM, EDP Sciences 2020
https://doi.org/10.1051/meca/2020006

Mechanics & Industry

Available online at:
www.mechanics-industry.org

Regular Article

Prediction of the optimal speed of an aerospace vehicle by aerothermochemical analysis of hypersonic flow during atmospheric re-entry

Rachid Allouche[1], Rachid Renane[1,*], and Rabah Haoui[2]

[1] Aeronautical Science Laboratory, Institute of Aeronautics & Space Studies, University of Blida 1, BP 270 Roud of Soumaa, Algeria
[2] Thermo-Energetic Department, University USTHB, Alger, Algeria

Received: 26 March 2019 / Accepted: 13 January 2020

Abstract. The objective of this work is to predict the optimal speed of an aerospace vehicle by aerothermochemical analysis of the hypersonic flow during atmospheric re-entry, out of equilibrium vibrational and chemical behind a detached strong shock. This study focuses on the influence of the ionization process that plays a significant role in the absorption of heat, because the characteristics of hypersonic flows are that molecules behind a strong shock wave become vibrationally excited, partially or completely dissociated and ionized depending on their bond energy, and the velocity of flow. On the other hand, we present the mathematical model that governs the flow of reactive gas mixture out of vibrational and chemical equilibrium that is composed of 79% nitrogen N_2 and 21% oxygen O_2. Conservation and relaxation equations (chemistry-vibration) are presented with particular importance to the expression of source terms. The numerical resolution method used is based on physical modeling, governed by the Euler equations, supplemented by the equations of chemical kinetics using the finite difference method. The results obtained are in good agreement with the specialized literature.

Keywords: Hypersonic / reactive flow / non-equilibrium / chemical dissociation / ionization / Euler equation / aerospace

1 Introduction

During atmospheric re-entry of space vehicles with super orbital speeds, air is considered composed of diatomic species (O_2 and N_2), the flow is hypersonic followed by aerodynamic braking which causes heating of the walls of these shuttles (see Fig. 1), this phase of flight is the most complex, to all the other phases of flight. The important kinetic energy involved can be transformed to thermal form and produce a significant heating, as well as the provocation of a particular aerothermal phenomenon like shockwave that envelops the spacecraft during re-entry [1]. The brutal rise in temperature just after the shock to the order of tens of thousands of degrees Kelvin causes physico-chemical processes that take place behind this shock such as vibrational excitation, dissociation of molecules, ionization, the electronic excitation of atoms and molecules as well as the effects of radiation. It is the formation of plasma from a mixture of eleven species: O, N, NO, O_2, N_2, O^+, N^+, NO^+, O_2^+, N_2^+, and e^-. The physico-chemical phenomena related to these conditions lead to a state of thermochemical imbalance [2,3]. Still poorly known which has a considerable influence on the convective and radiative heat fluxes, suffered by the walls of the spacecraft [4,10]. Thus, theoretical, experimental and numerical studies are developed throughout the world in order to understand these non-equilibrium phenomena (see Fig. 2). In these conditions of hypersonic flight, and for the calculation of internal energy, all modes of energy must be taken into account. The airflow around the spacecraft during their re-entry into the Earth's atmosphere may be the place of such phenomena; the energy exchanged by collisions is preponderant in an air flow behind an intense shock wave. The molecules acquire very quickly over a distance of a few free medium lengths of the translational-rotation energy in a volume of thickness, small enough to assimilate the shock wave to a surface of discontinuity, then gradually under the influence of collisions, the molecules become excited in vibration and dissociate and then ionize as a function of the translational-rotation energies [5]. For each energy transfer, time characterizing the state of equilibrium is defined.

* e-mail: r.renane@gmail.com

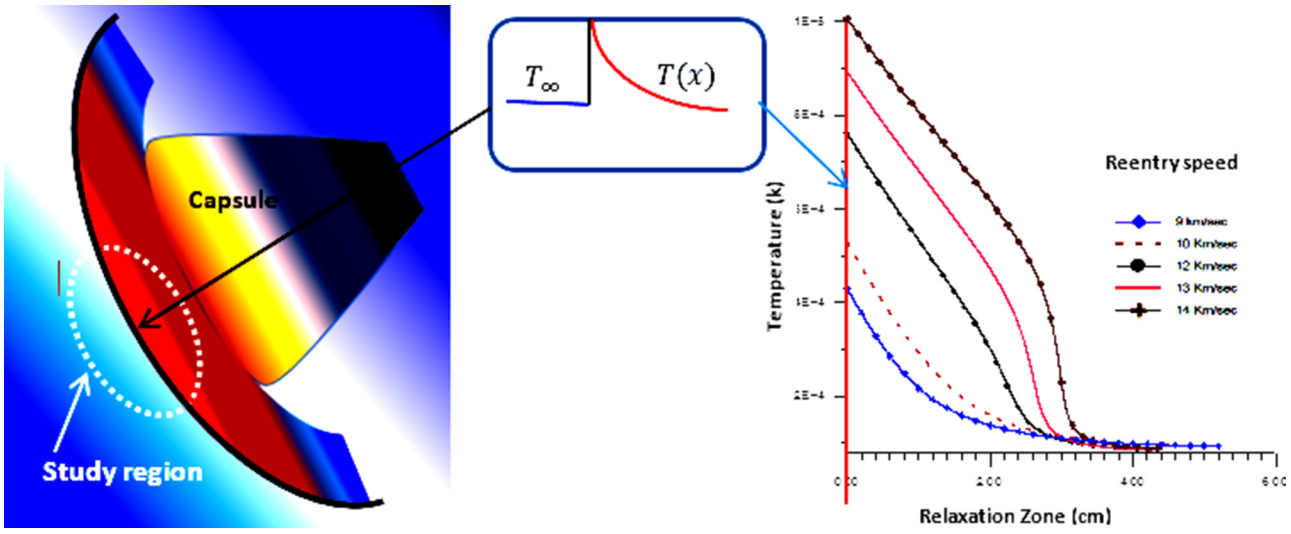

Fig. 1. Flight configuration during the atmospheric reentry with the thermal buckler and variation of flow temperature after the shock wave for different speeds of the capsules.

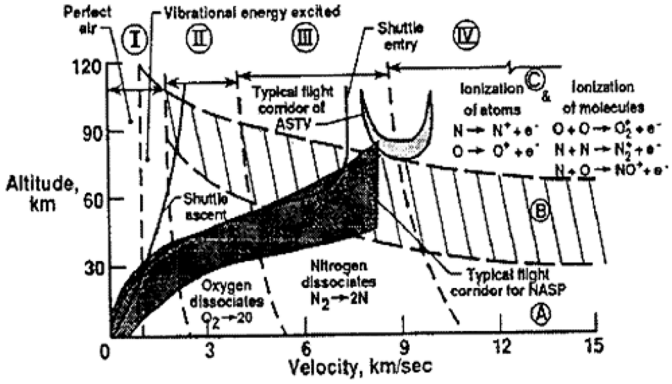

Fig. 2. Flow regimes and thermochemical phenomena during atmospheric re-entry [14].

The physico-chemical processes that appear after the strong shock wave, namely vibration, dissociation and molecular and atomic ionization according to their energy levels [6,11,16], allow us to calculate the thermodynamic parameters of the flow in the relaxation zone and more precisely the minimum equilibrium temperature of the fluid. The latter is related to initial atmospheric conditions and particularly to the speed of the fluid, which allows us to predict the optimal speed of the aerospace machine.

2 Modelisation of the hypersonic flow

2.1 Effect of velocity on the thermochemical characteristics of a flow

The sequence of phenomena that takes place behind an intense shock wave during atmospheric re-entry as shown in Figure 1: firstly, under the effect of the increase in temperature, the vibration of the molecules begins to take place [5,7,9], the oscillation amplifies and the atoms separate, it is the phenomenon of dissociation of the molecules [11,13]. If the temperature is still very high, the collision between atoms and molecules is very intense and gives rise to ionization [6,16]. We have the vibration of oxygen, then of nitrogen, dissociation of oxygen and then of nitrogen, as well as the ionization of atoms and molecules [6,11,13].

2.2 Modeling of thermodynamic properties

2.2.1 Hypotheses

According to statistical thermodynamics and under the hypothesis of the local thermodynamic equilibrium, makes it possible to establish the expressions of the energy stored by a particle on its various internal modes. The out of equilibrium thermodynamic flow is described here as a continuous medium (the Knudsen number $Kn \leq 10^{-3}$) [8,12] in which the pressure and the density are sufficiently large to define macroscopic quantities characterizing flow. The present study assumes a one-dimensional reactive flow. In the gaseous mixture, each species follows the state law of perfect gases, the fluid is considered to be Newtonian, and the viscosity and diffusion effects of the species are neglected. This hypothesis thus reduces the Navier-Stokes equations to those of Euler. In the total energy conservation equation, and in the electronic relaxation equation, the radiative heat flux is neglected. The thermodynamic imbalance in the ionized gas mixture induces two temperatures characterizing the energies of each mode (translational, vibrational) [7,9]. The rotation temperature of the molecules is supposed to be equal to the translation temperature of each species, since the translational and rotational characteristic times are sufficiently short, so that the temperatures of the latter equilibrate very rapidly.

2.2.2 The different modes of energy storage

The atoms are assimilated to rigid spheres, and the molecules are bound to these spheres by rigid springs as shown in Figure 3, where: RT : Rotation-translation energy exchanges; VT : Vibration-translation energy exchanges; ET: Electron free-translation energy exchanges; RR:

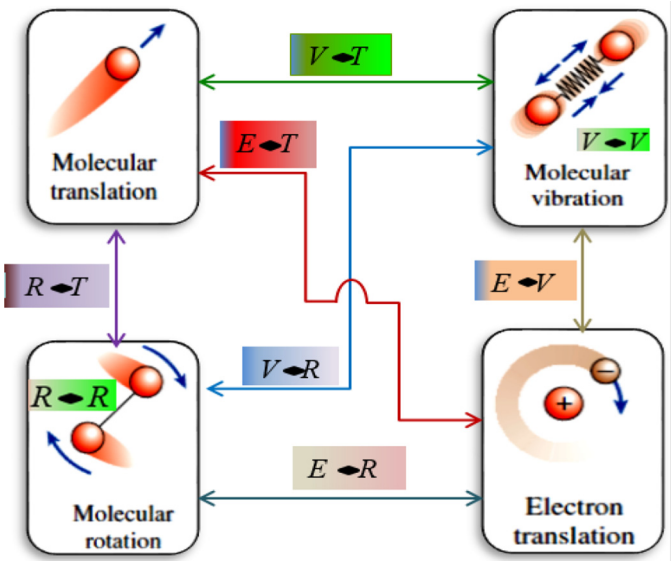

Fig. 3. Interchanges between different energy modes of an ionized gas.

rotation-rotation energy exchanges; VR: Vibration-rotation energy exchanges; E R: Free electron rotation energy exchanges; VV: Vibration-vibration energy exchanges; EV: free electron vibration energy exchanges.

3 Resolution method

The mathematical model used for simulation of reactive flow, hypersonic, one-dimensional and inviscid is based on the numerical solution of Euler equations with the equations of chemical kinetics. The discretization of differential equations of first order is based on the finite difference method where a very fine mesh is used in the relaxation zone in order to determine the flow at each grid position, replacing the derivatives by finite differences. These equations are written in a reference connected to the shock wave moving at constant speed as follows:

The conservation equations of the flow used by the references [1,4] are discretized in Section 4 of this work.

3.1 Modeling source terms

In the following, we present briefly, a chemical source (W_{CS}) and vibrational (W_{VS}) terms, thus the coupling phenomena CVD and CVDV.

3.1.1 Source term of chemical production (*WCS*)

The study of chemical kinetics allows us to express the source term of the equations of the reactive species evolution of a gaseous mixture at high temperature [12], a large number of chemical reactions will take place simultaneously (see Tab. 1). The equations for each reaction r are given by [2,10,11]:

$$\sum_{s=1}^{11} \nu'_{s,r} A_s \underset{K_{b,r}}{\overset{K_{f,r}}{\Leftrightarrow}} \sum_{s=1}^{11} \nu''_{s,r} A_s;\ r = 1-47 \tag{1}$$

where A_s: species $s7$; $\nu'_{s,r}$, $\nu''_{s,r}$: stoichiometric coefficients corresponding to reaction r and species s; $K_{f,r}$, $K_{b,r}$: the constants of the chemical kinetics (forward) and (backward).

The mass production rate of the chemical species will be written [13]

$$\omega_{cs} = M_s \sum_{r=1}^{47} \left(\nu''_{s,r} - \nu'_{s,r}\right) \times \left[K_{f,r} \prod_{s=1}^{11} \left[\frac{\rho_s}{M_s}\right]^{\nu'_{s,r}} - K_{b,r} \prod_{s=1}^{11} \left[\frac{\rho_s}{M_s}\right]^{\nu''_{s,r}}\right]. \tag{2}$$

The expressions of the chemical kinetics constants are as follows – (Park model):

$$K_f(T) = C\ T^n\ \exp\left(-\frac{\theta_d}{T}\right) \tag{3}$$

$$K_{eq}(T) = \exp\left(C_0 + C_1 z + C_2 z^2 + C_3 z^3 + C_4 z^4\right), \quad z = \frac{10000}{T} \tag{4}$$

$$K_b(T) = \frac{K_f(T)}{K_{eq}(T)}, \tag{5}$$

where K_{eq} is the equilibrium constant at temperature T.

Constants (C, n, C_0, C_1, C_2, C_3, C_4) are given by the Janaf tables [5].

3.2 Coupling chemistry – vibration

3.2.1 Influence of vibration on chemistry

Depending on the type of reaction, three types of chemistry/vibration coupling are generally considered in the literature: chemistry/vibration coupling for dissociation reactions (CVD), coupling for recombination reactions (CVR) and coupling for reactions of exchange (CVCE).

3.2.2 Coupling factor vibration – dissociation CVD

The more the vibratory state of a molecule is excited, the more it tends to dissociate. The vibration temperature therefore has an influence on the reactivity of a molecule. If the vibration temperature is greater than the translation temperature, then all the chemical reactions resulting from its dissociation are favored. The constants of dissociation reactions are multiplied by a factor $V(T, T_V)$ as a function of the translation temperature, the vibration temperature and a dummy temperature T_a related to the characteristic dissociation temperature of the molecule [5,8,10].

$$V(T, T_V) = (T^{q-1} T_v^{1-q})^n \frac{\exp(-\theta_d/T_a)}{\exp(-\theta_d/T)}, \tag{6}$$

Table 1. Kinetic model [8].

Number of reaction	Reaction	Energy released
	Dissociation of molecules	
$r = 1$ à 11	$O_2 + m \Leftrightarrow 2O + m$	5.12 ev
$r = 12$ à 22	$N_2 + m \Leftrightarrow 2N + m$	9.76 ev
$r = 23$ à 33	$NO + m \Leftrightarrow N+O+ m$	6.49 ev
	Exchange reactions	
$r = 34$	$N_2 + O \Leftrightarrow NO + N$	3.27 ev
$r = 35$	$NO + O \Leftrightarrow O_2 + N$	1.37 ev
$r = 36$	$O + {O_2}^+ \Leftrightarrow O_2 + O^+$	1.61 ev
$r = 37$	$N_2 + N^+ \Leftrightarrow N + {N_2}^+$	1.05 ev
$r = 38$	$O + NO^+ \Leftrightarrow NO + O^+$	4.43 ev
$r = 39$	$N_2 + O^+ \Leftrightarrow O + {N_2}^+$	1.94 ev
$r = 40$	$N + NO^+ \Leftrightarrow NO + N^+$	5.32 ev
$r = 41$	$O_2 + NO^+ \Leftrightarrow NO + O_2+$	2.82 ev
$r = 42$	$N + NO^+ \Leftrightarrow O + {N_2}^+$	3.09 ev
	Association ionization	
$r = 43$	$O + N \Leftrightarrow NO+ + e-$	2.79 ev
$r = 44$	$O + O \Leftrightarrow {O_2}^+ + e-$	7.01 ev
$r = 45$	$N + N \Leftrightarrow {N_2}^+ + e-$	5.88 ev
	Electron impact ionization	
$r = 46$	$O + e- \Leftrightarrow O+ + e- + e-$	13.78 ev
$r = 47$	$N + e- \Leftrightarrow N+ + e- + e-$	14.67 ev

m: Catalyst, r: reaction.

where, T_a: fictional temperature proposed by Park [5]

$$T_a = T^q\, T_v^{1-q} \tag{7}$$

and $q = 0.7$: Parck model parameter; θ_d: the characteristic temperature of dissociation, where

$$\theta_{d,\mathrm{N_2}} = 113085\,\mathrm{K},\ \ \theta_{d,\mathrm{O_2}} = 59380\,\mathrm{K}, \theta_{d,\mathrm{NO}} = 75500\,\mathrm{K}.$$

3.3 Source terms of vibration W_{VS}

When two molecules collide one gains (or loses) vibration energy that the other yields (or takes) as trans-rotation energy or vibration energy. To model the phenomena of vibration, we suppose that the diatomic species answer the hypothesis of the harmonic oscillator with a finite number of energy levels.

The term source of vibrational energy can be written as follows:

$$\omega_{V,S} = \omega_{VT,S} + \omega_{VE,S} + \omega_{VC,S} \tag{8}$$

with:
$\omega_{VT,S}$: energy exchange rate translation − vibration;
$\omega_{Ve,s}$: energy exchange rate electronic − vibration;
$\omega_{VC,s}$: energy exchange rate vibration − chemical.

3.3.1 Translation–vibration energy exchange

The energy exchange model between translation modes and vibration modes is described by the Landau-Teller formula, where vibrational transitions are assumed to occur only between neighboring levels. The rate of vibrational energy transfer is written as follows:

$$\omega_{VT,s} = \rho_s \frac{E^*_{vs}(T) - e_{v,s}(T_V)}{\tau_s} f_s, \tag{9}$$

where, f_s is Park's correction factor.

$$E^*_{vs} = \frac{R\theta_{vib\,s}}{\exp\left(\dfrac{\theta_{vib\,s}}{T}\right) - 1} \tag{10}$$

and $\theta_{vib\,s}$: is the characteristic temperature of vibration where:
$\theta_{vibs,\mathrm{N}_2} = 3395\,\mathrm{K}$, $\theta_{vibs,\mathrm{O}_2} = 2239\,\mathrm{K}, \theta_{vibs,\mathrm{NO}} = 2817\,\mathrm{K}$

$$\tau_s = \tau_{s_{(M,W)}} + \tau_{s\,(j,c)}. \tag{11}$$

The relaxation times used here are the times given by the Millikan and White formula $\tau_{s_{(M,W)}}$ with Park's correction term: $(\tau_{s(j,c)})$ [2,4,5] with, the vibrational relaxation time of the molecule s in the gas mixture is written [2,4]

$$\tau_{s_{M,W}} = \sum_j y_j / \sum_j (y_j/\tau_{sj}), \tag{12}$$

$$\tau_{sj} = \frac{1}{P}\exp(A_{sj}(T^{-1/3} - 0.015\mu_{sj}^{1/4}) - 18.42), \tag{13}$$

where P is the total pressure of the mixture expressed in atm

$$A_{sj} = 1.16 \times 10^{-3} \times {\mu_{sj}}^{1/2}\theta_{vib,j}^{4/3}$$

and

$$\mu_{sj} = \frac{M_s M_j}{M_s + M_j}$$

μ_{sj} is the reduced mass of the molar masses M_s and M_j, where y_j represents the molar fraction of a species in the mixture.

The expression of f_s is according to the temperatures behind the shock wave, it is given by [2,5]:

$$f_s = \left[\frac{T_{\mathrm{ch}} - T_{vs}}{T_{\mathrm{ch}} - T_{v,s,\mathrm{ch}}}\right]^{q_s - 1} \tag{14}$$

with

$$q_s = 3.5\mathrm{Exp}(-\theta_S/T_{ch}) \tag{15}$$

T_{ch}: temperature just behind the shock wave; $T_{v,s}$: vibration temperature of species s; $T_{v,s,ch}$: vibration temperature for the species s just behind the shock wave; θ_S: characteristic temperature of the molecule s, where: $\theta_{\mathrm{N}_2} = 5000\,\mathrm{K}$, $\theta_{\mathrm{O}_2} = 3350\,\mathrm{K}$ and $\theta_{\mathrm{NO}} = 4040\,\mathrm{K}$.

3.3.2 Electronic–vibration energy exchange

In addition to rotational and vibrational excitations, the collisions between a molecule and other particles can lead to electronic transitions of the molecule. The energy transfer rate between the electronic modes and the vibration modes is described by Lee in the same way as the Landau-Teller theory and is written [2]:

$$\omega_{Ve,s} = \rho_s \frac{E_{vs}^{**}(T_e) - e_{v,s}(T_V)}{\tau_{e,s}} \tag{16}$$

$$d\frac{\vec{F(w)}}{\mathrm{d}x} = \vec{\Omega}(w)\,, \tag{17}$$

where the vectors F and Ω represents conservative flows and source terms, respectively. These vectors are expressed as follows:

$$F(\omega) = \left\{\begin{array}{c} \rho\ u \\ P + \rho\ u^2 \\ u(\rho E + P) \\ \rho\ u \\ \rho_j e_{v,j} u \end{array}\right\} \tag{18}$$

$$\Omega\ (\omega\,) = \left\{\begin{array}{c} 0 \\ 0 \\ 0 \\ \omega_{\,c,s} \\ \omega_{\,v,j} + \omega_{\,c,j}\ e_{\,v,j} \end{array}\right\}. \tag{19}$$

4 Equation setting

The purpose of the equation setting is the calculation of the mass, and molar fractions of the different constituents as a function of their (x) displacement according to the variation of temperature as well as the source terms, because, the relation which links the mass fraction of the species (i) during its displacement by the term of production Wi is given by the relation (20).

$$d(\rho_S u)/dx = \omega_{C,S}. \tag{20}$$

At each (x) displacement, the quantity of mass, momentum, and quantity of energy of the flow are conserved. The system of the conservation equations for mass, momentum and energy is given as follows [17]:

$$\left.\begin{array}{l} \rho(i)\ u(i)\ =\ \rho(i+1)\ u(i+1) \\ P(i) + \rho(i)u^2(i) =\ P(i+1) + \rho(i+1)u^2(i+1) \end{array}\right\} \tag{21}$$

$$\left.\begin{array}{l} Cp_m(i)T(i) + \frac{1}{2}u(i)^2 + \sum\limits_{atom+ion} Y_S(i)h_{f,s}^0 \\ +\ \sum\limits_{diatom} Y_S(i)e_{vs}(i) =\ Cp_m(i+1)T(i+1) + \frac{1}{2}u(i+1)^2 \\ +\ \sum\limits_{atom+ion} Y_S(i+1)h_{f,s}^0 + \sum\limits_{diatom} Y_S(i+1)e_{vs}(i+1) \end{array}\right\} \tag{22}$$

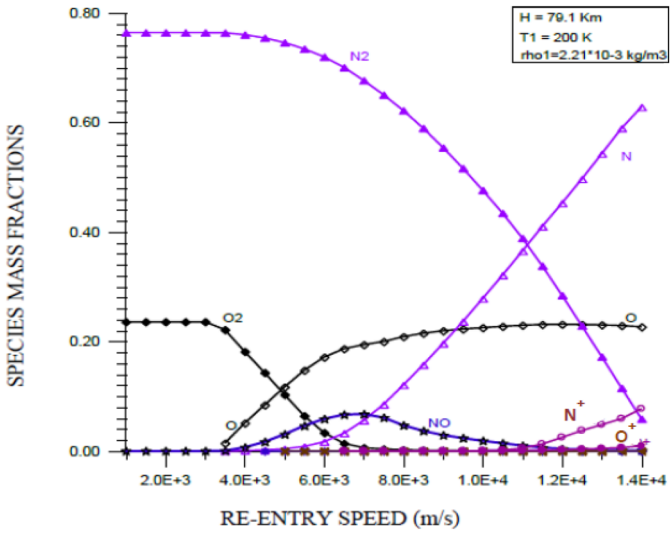

Fig. 4. Evolution of mass fractions as a function of the speed of re-entry.

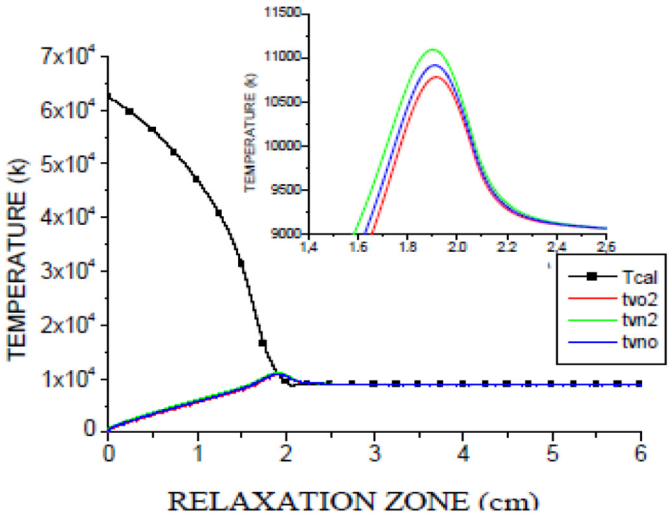

Fig 5. Variation of translational and vibrational temperatures behind the shock wave with conditions at infinity upstream: $U\infty = 11360$ [m/s], $T\infty = 195$ [k], $P\infty = 2$ [Pa].

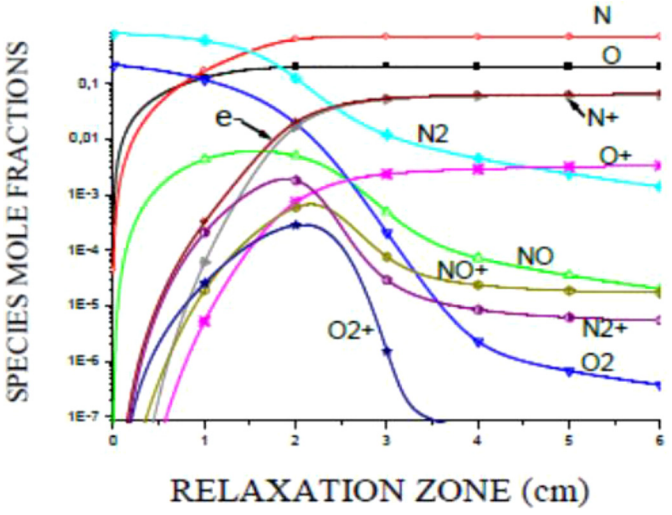

Fig 6. Variation of the molar fractions behind the shock wave with the conditions at infinity upstream: $U\infty = 11360$ [m/s], $T\infty = 195$ [k], $P\infty = 2$ [Pa].

The term $ev_s(i+1)$ is evaluated explicitly, using the evolution equation of the vibration energy as well as the finite differences that gives:

$$\left.\begin{aligned} &\frac{de_v}{dx} = \frac{1}{u.\rho_s}(\omega_{c,s}e_{v,s} + \omega_{v,s}) \\ &\text{and} \\ &\frac{de_v}{dx} = \frac{e_v(i+1) - e_v(i)}{\Delta x} \end{aligned}\right\} \quad (23)$$

which leads to:

$$e_v(i+1) = e_v(i) + \Delta x\left(\frac{1}{u(i).\rho_s(i)}(\omega_{c,s}e_v(i) + \omega_{V,s})\right). \quad (24)$$

5 Results and discussion

For the resolution of nonlinear equations describing a compressible fluid flow in chemical imbalance by the finite difference technique, a FORTRAN computation code was realized. It was admitted that the chemical model of the air is composed of eleven species. The vibratory energy modes are considered out of equilibrium and therefore the vibration temperature does not equal the translational-rotation temperature of the flow in the relaxation zone [5]. Several results can be presented by executing our code.

In Figure 4, we present the evolution of the mass fractions as a function of the re-entry speed, we note that the mass concentration of electrons and ions is not visible for speeds below 11 km/s. After this speed, we notice the birth of ions induced by the exchange reactions and associative ionization, which favors the rapid decrease of the temperature in the relaxation range.

Figure 5 shows respectively the evolution of the translational temperature and the vibration temperatures for the diatomic molecules. It is noted that the translational temperature is very important behind the shock, then it decreases regularly and rapidly under the effect of endothermic reactions, on the other hand, a rapid increase in temperatures T_{VO2}, T_{VN2} and T_{VNO} in the form of a bell then stabilizes at equilibrium with the temperature of the flow. There is good agreement between our results and those of T. Thierry et al. [8] for similar initial flight conditions.

Figure 6 illustrates the evolution of the molar concentrations of the eleven species in the relaxation range. The amount of (O_2, N_2) decreases from their initial values under the effect of dissociation reactions [11,13]. In addition, there is the formation of O, N and nitric oxide NO. Ionization occurs by the presence of electrons and ions (NO^+, N^+, N_2^+, O^+ and O_2^+). Note that our results obtained with a chemical model of 47 reactions (presented in Tab. 1) corroborate the results of Chull Park [8,12] with a model of 31 reactions (see Fig. 7), an infinitesimal

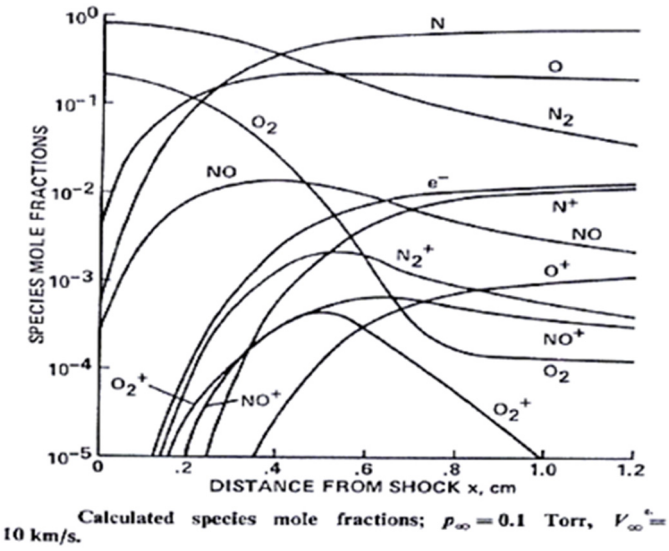

Calculated species mole fractions; $p_\infty = 0.1$ Torr, V_∞ = 10 km/s.

Fig 7. Results given by C. Park [8].

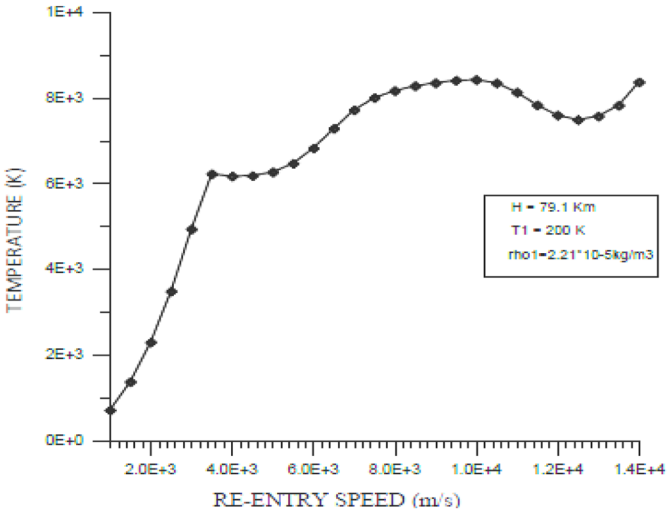

Fig. 9. Evolution of equilibrium temperature after shock as a function of entry speed.

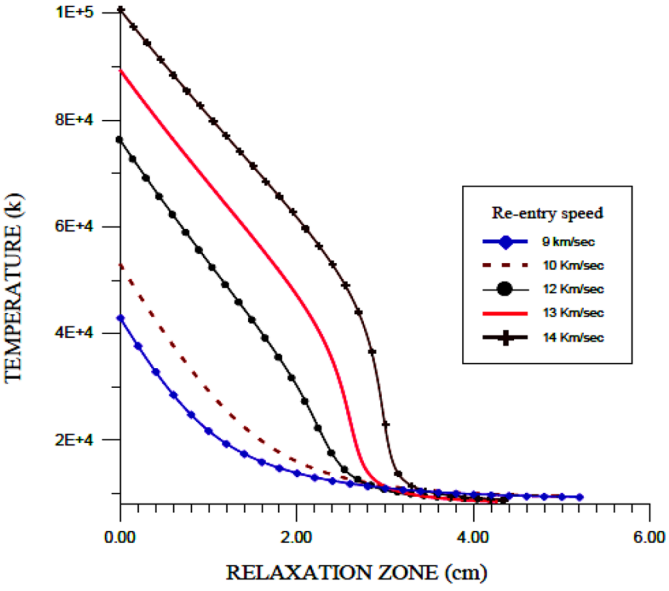

Fig. 8. Variation of the temperature in the relaxation range for different speeds at the altitude of 85 km.

difference is observed at the level of NO and N_2, and this is due to the number of additive associative reactions in our model.

The temperatures just behind the shock are variables (see Fig. 8). For example, when the speed is 9 km/s the reached temperature is 42 829 K, if the speed increases to 14 km/s the temperature behind the shock has the value of 100 626 K. For the first case the ionization is negligible, by against in the second case it is considerable. This is why we have equilibrium averaging the same temperatures. The temperature difference is absorbed by the ionization phenomenon [6]. Regarding the length of the relaxation range, it can be seen that the difference is not large.

Figure 8 shows the variation of the temperature in the relaxation range for different speeds at an altitude of 85 km. It is seen that the temperature variations have the same paces, strongly decreasing at the beginning because the reaction rates are fast, a large part of the thermal energy is used to cause dissociation and ionization. After, and since the temperature decreases, the reaction rates are slower and, therefore tend to a state of equilibrium. On the other hand, it is known that at high temperatures the gas is very agitated and the number of collisions is very large, which quickly favors dissociation and ionization, so that the equilibrium state is rapidly reached [6,7,9]. Our results in Figure 6 corroborate with C. Park results shown in Figure 7.

From the quantitative point of view, and from Figure 9, we can see directly the effect of the speed on the equilibrium temperature at the end of relaxation. For speeds less than 3 km/s the shape of the temperature variation is progressive, which means that no dissociation phenomenon has appeared.

From this limit, the variation of the temperature changes shape and varies according to the processes of dissociation and ionization, which will take place in the flow [11,13,16]. For example, when the speed is 9 km/s, the reached temperature is 42 829 K, if the speed increases to 14 km/s the temperature behind the shock has the value of 100 626 K. For the first case, the ionization is negligible, by against in the second case, it is considerable. This is why in equilibrium, and according to Figure 8, we have noticed that the equilibrium temperature is of the order of 8500 K for a speed of 9 km/s, against it is of 7300 K at the entry speed of 13 km/s, these gains in descent time, also in terms of the minimum equilibrium temperature reached due to the dominant ionization phenomenon at these conditions, this result allows us to deduce that the optimal re-entry speed of a spacecraft is about of 13 km/s.

Figure 10 shows that the concentrations of O_2 and N_2 are constant when the velocity is less than 3 km/s. The molar concentration of the electrons is clear in this figure, it increases as the speed of entry increases, the results of the latter shows that the curves have the same pace with reference [15] on all the regimes (see Fig. 11) and coincide with a certain gap near.

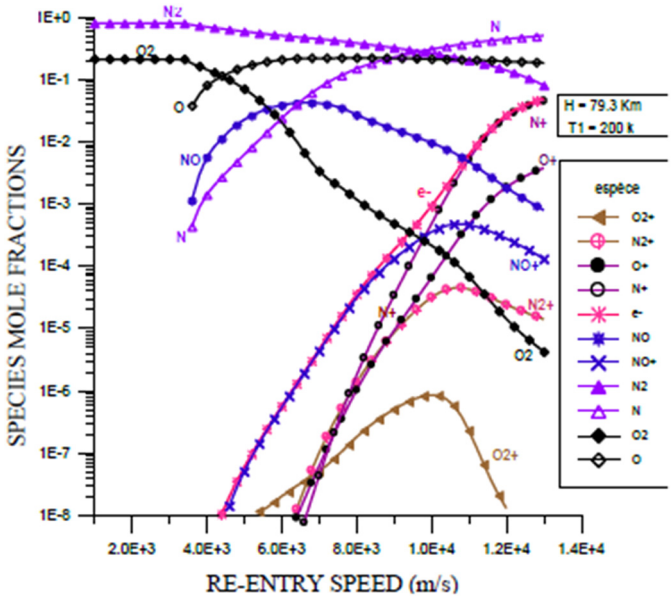

Fig. 10. Evolution of the molar fractions as a function of the entry speed.

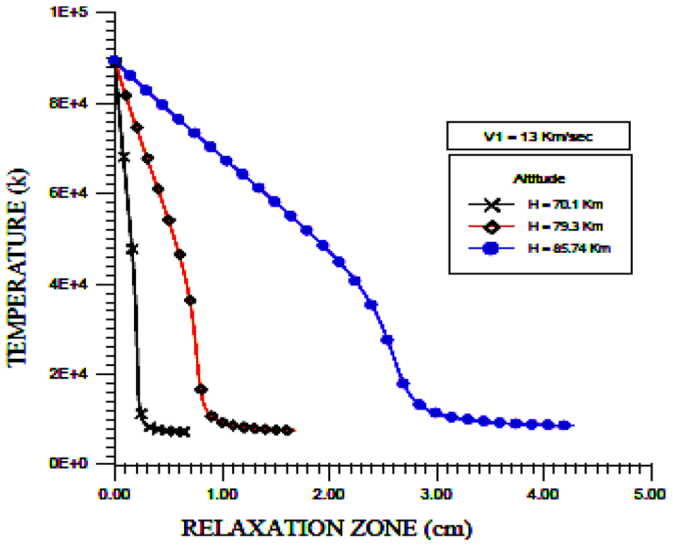

Fig. 12. Temperature variation in the relaxation range for different altitudes at a speed of 13 km/s.

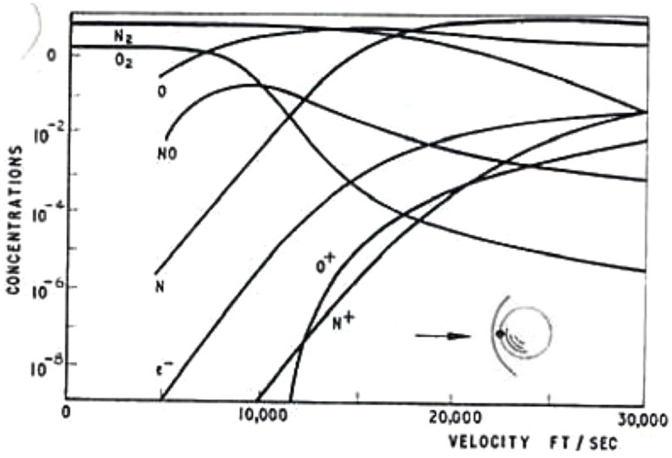

Fig. 11. Mole fraction distributions behind normal shock [15].

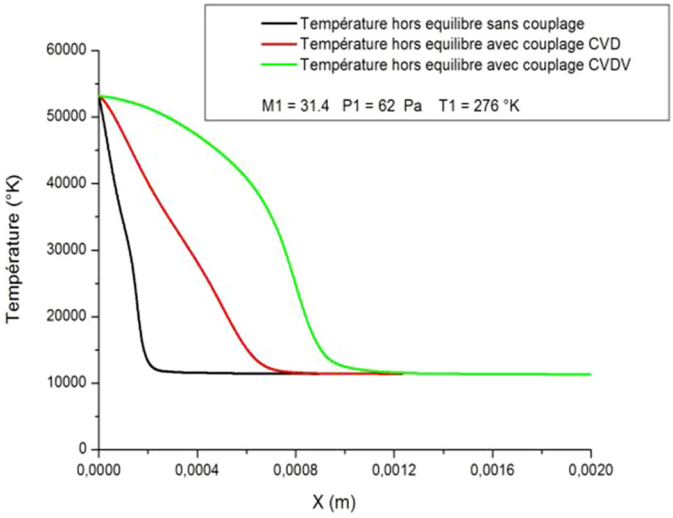

Fig. 13. Evolution of the transrotation temperature for the different modes at Mach $M = 31.4$.

Figure 12 shows the evolution of the temperature of the gas mixture in the relaxation range for different altitudes. The speed of the spacecraft is chosen equal to 13 km/s. It can be seen that the three temperature variations have the same paces, strongly decreasing at the beginning because the reaction rates are fast, a large part of the thermal energy is used to cause dissociation and ionization. After, and since the temperature decreases, the reaction rates are slower and therefore tend to a state of equilibrium. Only the difference between the three cases presented is in the length of the relaxation range. Note that more the altitude is higher, the relaxation range is largest (0.67 cm at 70 km become 4.27 cm at 85 km). This difference is caused by the difference in altitude pressure. It is known that at high pressures the gas is very agitated and the number of collisions is very large, which quickly promotes dissociation and ionization, therefore it quickly reaches the equilibrium state.

Figure 13 shows the transrotation temperature profile Ttr for different modes (without coupling with CVD and CVDV coupling). It is observed that immediately behind the shock wave, the translation temperature is very high, and then decreases to the equilibrium state. This decrease is much less rapid in the case with coupling, which initiates the zone of vibrational imbalance. If we try to compare the results obtained in the different modes, we find that the decrease in temperature just after the shock wave is different in some modes where in the CVDV mode is slower compared to the mode of CVD.

Where CVDV: coupling vibration dissociation vibration and CVD: coupling vibration dissociation.

6 Conclusion

The main objective of this work is the numerical simulation of a hypersonic flow out of equilibrium vibrational and chemical through a strong shock wave, in order to predict the optimal speed of an aerospace vehicle during the atmospheric re-entry. A computation code in FORTRAN is realized to solve the mathematical model that takes into account the physicochemical phenomena which appear in the relaxation zone like the vibration, the dissociation of the molecules and the ionization of the formed species [11]. The latter consist of eleven species (O, N, NO, O_2, N_2, O^+, N^+, NO^+, O_2^+, N_2^+). In this study we recalled the different interaction modes between the molecules, the thermodynamic properties, the partition functions at a high temperature flow, and exploiting the expressions of the thermodynamic properties of the individual chemical components for the purpose of determining the overall characteristics of the reaction mixture. Among the main conclusions of this study:

From the quantitative point of view, and from Figure 8, we can see directly the effect of the speed on the equilibrium temperature at the end of relaxation zone. When the speed is 9 km/s the reached temperature is 42 829 K, if the speed increases to 14 km/s the temperature behind the shock decreases to the value of 10 626 K. For the first case the ionization is negligible by cons in the second case it is considerable. On the other hand, and according to Figure 9, we notice that the equilibrium temperature is of the order of 8500 K for a speed of 9 km/s, it becomes 7300 K with the speed of entry of 13 km/s, this gain in descent time and also in terms of minimum equilibrium temperature reached is due to the ionization phenomenon, that dominates these conditions because the ionization reactions have the endothermic nature, this result allows us to deduce that optimal speed of re-entry of a spacecraft is of the order of 13 km/s. The previously mentioned points have an important role to reduce quickly the temperature of flow after the shock and reduce the relaxation zone, and reach quickly the equilibrium in order to weaken the influence of impact temperature of flow on the wall of space vehicles [6].

The authors acknowledge Khawla Sid-Ahmed and Trik Meriem, English teachers at the University of Blida1 for granting time to correct and prepare this manuscript.

References

[1] G.V. Candler, P.K. Subbareddy, I. Nompelis, Decoupled implicit method for aerothermodynamics and reacting flows, AIAA J. **51**, 1245–1254 (2013)
[2] A. Abdelaziz, Modélisation d'une écoulement hypersonique de CO en déséquilibre physico-chimiques et radiatif derrière une onde de choc, Thèse Doctorat de L'université de Provence (Aix-Marseille I), 2002
[3] G. Tchuen, D.E. Zeitoun, Effects of chemistry in nonequilibrium hypersonic flow around blunt bodies, J. Thermophys. Heat Transf. **23**, 433–442 (2009)
[4] K. Koffi-Kpante, Etude des phénomènes de déséquilibre thermochimique dans la couche de choc radiative de l'atmosphère simulée de TITAN, Thèse Doctorat de L'université de Provence (Aix-Marseille I), 1996
[5] R.C. Millikan, D.R. White, Systematics of vibrational relaxation, J. Chem. Phys. **39**, 3209–3213 (1963)
[6] T. Soubrié, Prise en compte de l'ionisation et du rayonnement dans la modélisation des écoulements de rentrée terrestre et martienne, Thèse Doctorat de l'Ecole nationale supérieure de l'aéronautique et de l'espace, 2006
[7] V. Casseau, T.J. Scanlon, R.E. Brown, Development of a two-temperature open-source CFD model for hypersonic reacting flows, AIAA Paper 2015-3637, 2015
[8] C. Park, On convergence of computation of reacting flows, AIAA 1985-0247, 1985
[9] V. Casseau, D.E. Espinoza, T.J. Scanlon, R.E. Brown, A two-temperature open-source CFD model for hypersonic reacting flows, part two: multi-dimensional analysis, Aerospace **3**, 45 (2016)
[10] J.M. Lamet, Transferts radiatifs dans les écoulements hypersoniques de rentrée atmosphérique terrestre, Thèse Doctorat de L'Ecole Centrale Paris, 2009
[11] T. Thierry, et al. Coarse-grain model for internal energy excitation and dissociation of molecular nitrogen, Chem. Phys. **398**, 90–95 (2012)
[12] C. Park, Assessment of two- temperature kinetic model for ionizing air, NASA Ames Research Center, Moffett Field, California, July 1989
[13] T.E. Magin, M. Panesi, A. Bourdon, R.L. Jaffe, D.W. Schwenke, Coarse-grain model for internal energy excitationand dissociation of molecular nitrogen, Chem. Phys. **398**, 90–95 (2012)
[14] J.D. Anderson Jr., Hypersonic and high-temperature gas dynamics, AIAA Education series, 2006
[15] R.N. Cox, L.F. Crabtree, Elements of hypersonic aerodynamics, The English Universities Press LTD, London, 1973
[16] G. Candler, The computation of weakly ionized hypersonic flow in thermo-chemical nonequilibrium, Dissertation, Stanford University, June 1988
[17] R. Allouche, R. Haoui. R. Renane, Numerical simulation of reactive flow in non-equilibrium behind a strong shock wave during re-entry into earth's atmosphere, Mech. Ind. **15**, 81–87 (2014)

Cite this article as: R. Allouche, R. Renane, R. Haoui, Prediction of the optimal speed of an aerospace vehicle by aerothermochemical analysis of hypersonic flow during atmospheric re-entry, Mechanics & Industry **21**, 208 (2020)